Acta Oceanol. Sin., 2015, Vol. 34, No. 3, P. 115–124
DOI: 10.1007/s13131-015-0627-6
http://www.hyxb.org.cn
E-mail: hyxbe@263.net

A wave energy resource assessment in the China's seas based on multi-satellite merged radar altimeter data

WAN Yong[1,2,3], ZHANG Jie[2], MENG Junmin[2], WANG Jing[1]*

[1] College of Information Science and Engineering, Ocean University of China, Qingdao 266100, China
[2] First Institute of Oceanography, State Oceanic Administration, Qingdao 266061, China
[3] College of Information and Control Engineering, China University of Petroleum, Qingdao 266580, China

Received 20 June 2014; accepted 11 October 2014

Abstract

Wave energy resources are abundant in both offshore and nearshore areas of the China's seas. A reliable assessment of the wave energy resources must be performed before they can be exploited. First, for a water depth in offshore waters of China, a parameterized wave power density model that considers the effects of the water depth is introduced to improve the calculating accuracy of the wave power density. Second, wave heights and wind speeds on the surface of the China's seas are retrieved from an AVISO multi-satellite altimeter data set for the period from 2009 to 2013. Three mean wave period inversion models are developed and used to calculate the wave energy period. Third, a practical application value for developing the wave energy is analyzed based on buoy data. Finally, the wave power density is then calculated using the wave field data. Using the distribution of wave power density, the energy level frequency, the time variability indexes, the total wave energy and the distribution of total wave energy density according to a wave state, the offshore wave energy in the China's seas is assessed. The results show that the areas of abundant and stable wave energy are primarily located in the north-central part of the South China Sea, the Luzon Strait, southeast of Taiwan in the China's seas; the wave power density values in these areas are approximately 14.0–18.5 kW/m. The wave energy in the China's seas presents obvious seasonal variations and optimal seasons for a wave energy utilization are in winter and autumn. Except for very coastal waters, in other sea areas in the China's seas, the energy is primarily from the wave state with 0.5 m$\leqslant H_s \leqslant$4 m, 4 s$\leqslant T_e \leqslant$10 s where H_s is a significant wave height and T_e is an energy period; within this wave state, the wave energy accounts for 80% above of the total wave energy. This characteristic is advantageous to designing wave energy convertors (WECs). The practical application value of the wave energy is higher which can be as an effective supplement for an energy consumption in some areas. The above results are consistent with the wave model which indicates fully that this new microwave remote sensing method altimeter is effective and feasible for the wave energy assessment.

Key words: China's seas, multi-satellite merged altimeter data, wave energy resources, assessment, wave power density

Citation: Wan Yong, Zhang Jie, Meng Junmin, Wang Jing. 2015. A wave energy resource assessment in the China's seas based on multi-satellite merged radar altimeter data. Acta Oceanologica Sinica, 34(3): 115–124, doi: 10.1007/s13131-015-0627-6

1 Introduction

The ongoing development of human society and the economy is increasing the demand for energy. The reserves of some conventional fossil energy sources, such as petroleum, natural gas and coal, are limited and will be rapidly exhausted in the coming decades (Bai, 2006). In addition, carbon dioxide emissions from the conventional fossil energy sources lead to global warming. The lack of resources and pollution from the conventional energy is an important issue for all countries. Thus, the development of novel renewable energy sources is an urgent requirement for economical and societal progress. Many countries have conducted a research on the exploitation and utilization of a green renewable energy. There are several abundant renewable energy sources, including ocean wind energy, tidal energy, wave energy, current energy, thermal gradient energy and ocean salinity energy, in the oceans, which cover approximately 71% of the earth's surface (Guan, 2011). The wave energy has the greatest potential and is the most valuable type of the ocean energy because it will only slightly affect the environment and it is a form of mechanical energy. Previous work has estimated that the theoretical wave energy in the oceans is approximately 1 TW, which is hundreds of times larger than the power generated around the world (Li et al., 2010). The exploitation and utilization of the wave energy resources are an important strategy for solving energy problems that are caused by the lack of conventional energy resources and the environmental problems that are caused by carbon emissions.

Before exploitation, a reliable assessment of the wave energy resources, including the temporal and spatial distribution, seasonal variation and reserves, must be performed, which is called a wave energy assessment. The wave energy assessments have been performed by researchers in several countries. Early wave energy assessments were primarily based on the in situ observation, which do not provide long-term and large-scale results (Quayle and Changery, 1981). Owing to the development of ocean technology, previous studies have assessed the wave

Foundation item: The Ocean Renewable Energy Special Fund Project of the State Oceanic Administration of China under contract No. GHME2011ZC07; the Dragon III Project of the European Space Agency and Ministry of Science and Technology of China under contract No. 10412.
*Corresponding author, E-mail: wjing@ouc.edu.cn

energy resources in several regions of the world using wave models, including numerical wave models (Pontes, 1998; Pontes et al., 2005; Cornett, 2008; Folley and Whittaker, 2009; Stopa et al., 2011; Arinaga and Cheung, 2012; Zheng et al., 2014). The development of a microwave remote sensing technology has introduced a new method for collecting a wave observation. Moreover, several wave energy resource assessment studies have used remote sensing data. On the basis of the analysis of 2-year T/P satellite altimeter data, Barstow et al. (1998) obtained a wave energy evaluation in several hundred discrete points along global coastline deep water. Pontes and Bruck (2008) carried out the wave energy assessment using the remote sensed data and revealed successfully that altimeter data and SAR data are effective for the wave energy assessment. In general, studies for the wave energy assessment by the remote sensing data are scarce.

The offshore areas of China are located in the East Asia monsoon climate zone. Northerly winds prevail during the winter; strong gales with cold waves are common. Southerly winds prevail during the summer, and the region is often affected by typhoons. In this region, ocean waves are strong; therefore, wave energy resources are abundant, which is advantageous for the exploitation and utilization of the wave energy resources (Wang, 1984). The wave energy resource assessments have been performed in China since the 1980s. Wang (1984) analyzed the distributions and variations of wave energy characteristics in nearshore areas of China using *in situ* wave data from ocean stations. Wang and Lu (1989) performed a wave energy zoning study for rural coastal areas in China, which is the most comprehensive, systematic and scientific assessment of the wave energy resources in coastal areas of China to date. Ren et al. (2008) and Ren et al. (2009) established an assessment system for ocean wave information resources and analyzed the wave energy in the Zhejiang Shengshan coastal area. Furthermore, Zheng et al. (2011), Zheng and Li (2011), Zheng et al. (2012), Zheng and Pan, et al. (2013) and Zheng and Su, et al. (2013) comprehensively and systematically assessed the wave energy resources in the China's seas using high-resolution wave fields simulated with the WAVEWATCH-III and SWAN wave models. These studies have played an important role in promoting the development of the wave energy resources in the China's seas. In addition, Zheng and Pan (2014) analyzed the global ocean wind energy resource based on CCMP (cross-calibrated, multiplatform) wind field data with resolution 0.25°×0.25° for the period 1988–2011. This research fills a gap in our knowledge in this field and provides an important reference for the wave energy resource assessment.

Radar altimeters can provide a long-term and extensive *in situ* wave observation that are different from wave model data. The altimeter could provide an accurate significant wave height which has been widely used in an ocean wave research field. On the one hand, altimeter data can be as a verification data set for the simulated results from a wave model (Stopa et al., 2011; Zheng et al., 2012). On the other hand, the altimeter data always can be as *in situ* data and be assimilated into wave models to improve the accuracy of the wave models (ECMWF, 2013; Hsu et al., 2011). It can be seen that the altimeter can provide high-precision wave data and represent a novel method for collecting wave observations and conducting the wave energy assessment. The wave energy assessment in China trailed assessments in other countries. Moreover, inadequate methods have been used for making the wave observation. The wave energy assessment has not been performed using the remote sensing data. In this study, we calculated several characteristic wave energy quantities using AVISO multi-satellite merged altimeter wave data from CNES and CLS. The temporal and spatial wave energy distributions in the China's seas were evaluated by considering a wave power density, an energy level frequency, a stability, a total wave energy and the distribution of the total wave energy density according to the wave state. This study is the first to assess the wave energy in the China's seas using the altimeter data.

2 Data sets and methodology

2.1 *Data sets*

2.1.1 *AVISO multi-satellite merged altimeter data*

Radar altimeters can provide relatively accurate significant wave height and wind speed data. The European Center for Medium-range Weather Forecasts (ECMWF) and the French Research Institute for Exploitation of the Sea (Ifremer) compared the measurements from several altimeters with buoy data and wave model data and found that the significant wave heights and wind speeds retrieved from altimeters are accurate; root mean square errors (RMSEs) were less than 0.5 m for the significant wave height and less than 2 m/s for the wind speed (Queffeulou et al., 2010; Abdalla et al., 2008). Moreover, the altimeter data have been considered accurate and are widely used to verify the wave model data (Stopa et al., 2011; Arinaga and Cheung, 2012; Zheng and Li, 2011). Thus, significant wave height and wind speed data from altimeters are reliable. There are limitations when a single altimeter is used to make observation in the coastal waters of China. In this paper, AVISO multi-satellite merged data were used to increase the coverage area of the China's seas.

The AVISO data from CNES and CLS (2010) are from several altimeters, such as Jason-1, ENVISAT, Jason-2 and Cryosat-2. The near-real-time significant wave height and wind speed data selected for this study were from September 2009 to August 2013 and encompassed 10°–41°N and 105°–129°E; the spatial and temporal resolutions were 1°×1° and 1 d, respectively. This data set was primarily used to provide wave fields data for the wave energy assessment.

Because the AVISO multi-satellite merged altimeter data have a lower spatial resolution, in order to obtain the detailed assessment for wave energy, Kring interpolation method was used to acquire a higher spatial resolution in this study. This method is also called a space autocovariance optimal interpolation method which is an optimal interpolation method named by Krige D G who is a mining engineer from South Africa. This method is widely used in some fields such as underground water simulation, soil cartography and so on which is a valuable gridded method for geological statistics. This method can provide a linear unbiased estimation for a research object.

2.1.2 *Buoy data*

Buoys are an important and accurate source of the *in situ* data for a wave observation that are often used to verify the results of other methods. This study used buoy data from five buoys located in the Bohai Sea, the Yellow Sea and the East China Sea during the GHME project in 2012. Table 1 shows the buoy specifications, which include three buoys of the Chinese Academy of Sciences (CAS), two wave dragon (AWAC) buoys. The data are from April 2012 to January 2013 and were collected at 10 or 30 min intervals. All of the buoys were located in nearshore areas where the water depths are less than 50 m. This data set was

Table 1. Buoy specifications

Buoy station ID	North latitude/(°)	East longitude/(°)	Water depth/m	Data period	Maintenance	Buoy type	General location
kzscd	38.058 8	120.654 1	14	Apr. 2012 to Jan. 2013	GHME group	AWAC buoy	Changdao coast
010	35.818 0	120.215 8	26	Apr. 2012 to Dec. 2012	GHME group	CAS buoy	Lingshan Island coast
NO.1WAVE-4	31.404 0	122.491 5	22	Apr. 2012 to Jan. 2013	GHME group	AWAC buoy	Chongming Island coast
011	30.550 0	122.366 7	26	Apr. 2012 to Dec. 2012	GHME group	CAS buoy	Daqushan coast
kzszs	29.752 7	122.750 0	42	Apr. 2012 to Dec. 2012	GHME group	CAS buoy	Zhoushan coast

primarily used to illustrate the necessity to calculate the wave power density by water depth model (WD-model) and practical application value for developing the wave energy.

2.1.3 *ERA-Interim reanalysis data*

The European Center for Medium-range Weather Forecasts (ECMWF) is one of main data reanalysis centers. ERA-Interim is the latest global atmosphere numerical reanalysis data set that has been provided by the ECMWF for global users. ERA-Interim provides highly accurate global wave field data, including the significant wave height and the energy period (T_e, s). Several comparisons and verifications of the wave fields from the buoys and reanalysis data have been presented in ECMWF technical memoranda. The RMSE of the significant wave height data is 0.395 m, and the RMSE of the energy period data is 0.730 s. These previous results show that the ERA-Interim wave field data are very accurate①. Therefore, the ERA-Interim energy period data set was selected to represent the true values for the altimeter mean wave period inversion in this study.

2.2 *Methodology*

The wave power density is the most important characteristic for the assessment of wave energy resources. This parameter has been typically calculated in recent studies by integrating model spectra based on numerical wave models. In this case, the wave power density (P_w) of a unit wave crest length is calculated by

$$P_w = \rho g \int_0^{2\pi}\int_0^{\infty} c_g(f,d)S(f,\theta)\mathrm{d}f\mathrm{d}\theta, \tag{1}$$

where ρ is the density (kg/m^3) of sea water; g is the acceleration (m/s^2) of gravity; c_g is the group velocity (m/s) of the wave energy propagation; $S(f, \theta)$ is the wave spectrum, f is the wave frequency (Hz) and θ is the direction (°) of the wave propagation; and d is the water depth (m) (Iglesias et al., 2009).

The empirical equation (EM-model) used to calculate the wave power density for offshore deep water areas is defined as

$$P_w \approx 0.5H_s^2T_e. \tag{2}$$

In deep water, the P_w values calculated from Eq. (2) are accurate which have been adopted by Zheng (Zheng et al., 2011; Zheng and Li, 2011; Zheng et al., 2012; Zheng and Pan, et al., 2013) However, in shallow or medium water depths, we must consider nearshore effects when calculating the wave power density, including refraction, shoaling, bottom dissipation and sheltering by the coastline or adjacent islands (Iglesias et al., 2009). In this situation, P_w is often calculated using Eq. (1). Unfortunately, the altimeter data cannot provide the wave spectrum; therefore, P_w cannot be calculated using the spectra integration method.

Several studies have shown that large areas between 50 and 200 km offshore in the China's seas have shallow and medium water depths of less than 50 m (figure omited). Although the altimeter data are not accurate within 50 km offshore (Yang, 2009), but some altimeter observation areas outside 50 km offshore where we can obtain accurate values are still located in shallow water areas. Thus, we must consider shoaling when calculating P_w.

To address this situation, a parametric model of P_w that considers the water depth (WD-model) was introduced. Wang and Lu (2009) indicated that P_w is equivalent to the hydrodynamic pressure (p) on a vertical plane that is orthogonal to the propagation direction multiplied by the velocity (u) of a water particle passing through the vertical plane, which can be calculated as follows:

$$P_w = \frac{1}{T}\int_0^T\int_{-d}^0 (p+\rho gz)u\mathrm{d}t\mathrm{d}z, \tag{3}$$

where t is the time (s); T is wave period (s) and z represents the water depth (m). We can integrate Eq. (3) over the wave period and the water depth. Therefore, P_w can be calculated using

$$P_w = \overline{E}c_g = \overline{E}\left(\frac{gT_e}{2\pi}\tanh kd\right)P_*, \tag{4}$$

where $\overline{E} = (1/16)\cdot\rho gH_s^2$, is the wave energy density (J/m^2); k=2π/λ, is the wavenumber (m^{-1}), λ is the wavelength (m); and $P_* = \frac{1}{2}\left(1+\frac{2kd}{\sinh 2kd}\right)$.

In the deep water (i.e., d/$\lambda\geqslant$1/2, P_*=1/2 and tanhkd≈1 were included in Eq. (4) and rearranged), P_w can be calculated as

$$P_w = \frac{\rho g^2}{64\pi}H_s^2T_e \approx 0.5H_s^2T_e, \tag{5}$$

which is the same as Eq. (2).

In the shallow water (i.e., d/λ<1/20, P_*=1 and tanhkd≈2πd/λ were included in Eq. (4) and rearranged), P_w can be calculated as

$$P_w = \frac{\rho g}{16}H_s^2\sqrt{gd}. \tag{6}$$

For medium water depths (i.e., 1/20≤d/λ<1/2), we must consider the shallow water correction. P_w can be calculated as

$$P_w = \overline{E}\left(\frac{gT_e}{2\pi}\tanh kd\right)\left[\frac{1}{2}\left(1+\frac{2kd}{\sinh 2kd}\right)\right]. \tag{7}$$

The water depth and the wavelength are necessary for determining the appropriate conditions and for calculating P_w. The water depth data were obtained from the University of Califor-

① Bidlot J R. 2012. Comparison of ECMWF re-analyses with *in-situ* wind and wave data. ECMWF Technical Memorandum

nia San Diego (UCSD) website and have a spatial resolution of 1′×1′ (Smith and Sandwell, 1997). The wavelength is estimated using the mean wave period; the relationship according to a sine wave theory is

$$\lambda = \frac{g}{2\pi} T_e^2. \tag{8}$$

However, Wen and Yu (1985) indicated that to obtain more accurate results, wavelength cannot be directly calculated from Eq. (8). Instead, we must multiply Eq. (8) by an empirical coefficient (0.87). Thus, wavelength can be calculated using

$$\lambda = 0.87 \frac{g}{2\pi} T_e^2. \tag{9}$$

Because the water depths in most sea areas of China are shallow, the accurate values of P_w must be obtained from the WD-model. In this section, the differences between calculating P_w in shallow waters using the WD-model and the EM-model are discussed using the buoy data from Stas No. 1 WAVE-4 and 011. A comparison of the monthly average P_w values calculated using these two models is shown in Fig. 1; blue denotes the WD-model results, and brown denotes the EM-model results. The results show that the P_w values predicted by the EM-model are less than those from the WD-model in shallow waters. Moreover, the results also suggest that as P_w increases (i.e., higher wave conditions), the difference between the models increases. To further examine the relationship between this difference and P_w, the results from these two buoys were categorized according to the P_w values, which is shown in Table 2, where the mean bias is the average of $P_{w\text{-}WD}-P_{w\text{-}EM}$. Table 2 indicates that the bias increases as P_w increases, the total mean bias is 0.57 kW/m, and the total RMSE is 1.47 kW/m, which increases with increasing wave conditions. Therefore, calculating P_w using the WD-model in shallow waters improves the accuracy of the P_w estimates in shallow waters.

Table 2. Statistics categorized according to the P_w values for the data from buoy stations No.1 WAVE-4 and 011

P_w/kW·m^{-1}	0–5	5–10	10–15	15–20	20–25	Total
Mean bias/kW·m^{-1}	0.08	0.46	0.99	1.65	2.40	0.57
RMSE/kW·m^{-1}	0.14	0.57	1.12	1.80	2.52	1.47

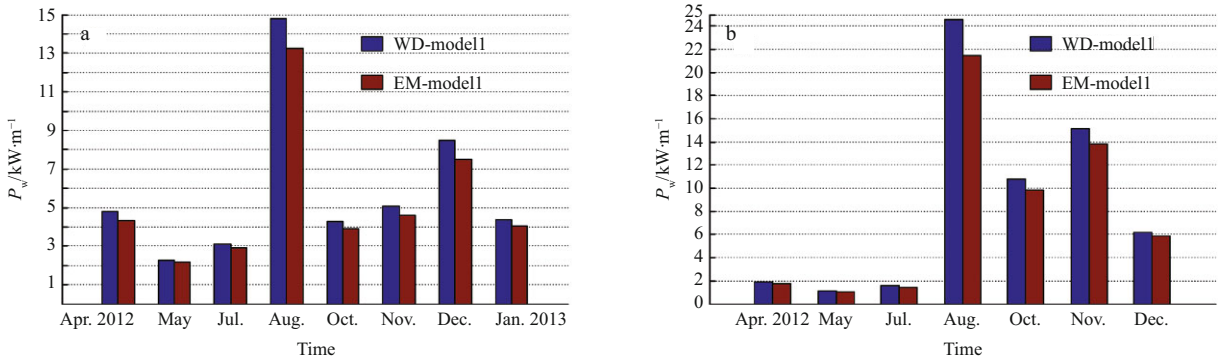

Fig. 1. Comparison of the monthly average P_w values calculated using the WD-model and the EM-model for buoy Stas No. 1 WAVE-4 (a) and 011 (b).

3 Wave period inversion and validation

The altimeter data set can provide relatively accurate significant wave height (H_s) and wind speed data; however, the data set cannot provide energy period, which is an important parameter for calculating P_w. energy period is often obtained by inversion modeling. Many inversion models have been developed, including the CS91 model, the H98 model, the G03 model, the Quilfen model, the Mackay model and the quartic polynomial empirical model (Challenor and Srokosz, 1991; Hwang et al., 1998; Gommenginger et al., 2003; Quilfen et al., 2004; Mackay et al., 2008; Miao et al., 2012). These models are all based on specific altimeter data and are suitable for specific oceanic areas. Several novel mean wave period inversion models fitted to multialtimeter satellites have been established using AVISO data and ERA-Interim data, including the polynomial model (PQ-AVISO-model), the polynomial subsection model (PQP-AVISO-model) and the BP neural network model (MWP-NN-model).

3.1 *Model development*

The studies of Wang (2006) and Miao et al. (2012) were foundations for the development of polynomial models. Wang (2006) presented the following relationship between the a nondimensional wave height and a wave age:

$$1.44 \frac{gT_z}{2\pi U_{10}} = \alpha \left(\frac{gH_s}{U_{10}^2} \right)^{\beta}, \tag{10}$$

where the nondimensional wave height is in the parentheses, the left hand side is the wave age; T_z is the zero-crossing mean wave period(s) (T_z=0.801 7T_e) (Li, 2007); and U_{10} is the wind speed (m/s). On the basis of ERA-40 and Jason-1 altimeter data, Miao et al. (2012) develop a quartic polynomial empirical model for the wave period inversion. On the basis of previous studies, the polynomial model is constructed as follows:

$$1.44 \frac{gT_z}{2\pi U_{10}} = \sum_{i=1}^{n} a_i \left(\frac{gH_s}{U_{10}^2} \right)^i + C. \tag{11}$$

The modeling data set was created using the AVISO data and ERA-Interim data from 2011, and the polynomial coefficients were fitted using the least squares method. The QP-AVISO-model was subsequently developed. The modeling data set was sectioned according to significant wave height. Then, the PQP-AVISO-model was formulated. The RMSE is the lowest when i is 5.

A BP neural network model was adopted to establish a neural network model for zero-crossing mean wave period. The same data set used previously was also used to calculate the nondimensional wave height (input) and the wave age (output). The neural network was trained using a LM method. Thereafter, the MWP-NN-model was established.

Furthermore, in order to verify the accuracy of models established in this paper, a quartic polynomial empirical model (Miao-QP-model), a quartic polynomial subsection empirical model (Miao-PQP-model) by Miao et al. (2012) and H98-model by Hwang et al. (1998) were selected to compare with three models in this paper.

3.2 *Validation*

The validation data set was created from the AVISO data and ERA-Interim data from 2012. Comparisons were carried out between three models in this paper and models by Miao et al and Hwang et al. The results are shown in Fig. 2. In order to evaluate the accuracy of inversion models through the compared results, we employ some accuracy indexes such as:

(1) Root mean square error (RMSE, $e_{\rm rms}$), which can be calculated using:

$$e_{\rm rms}=\sqrt{\frac{1}{n}\sum_{i=1}^{n}\left(y_i-x_i\right)^2}; \tag{12}$$

(2) Bias (b), which can be calculated using:

$$b=\overline{y}-\overline{x}; \tag{13}$$

(3) Correlation coefficient (CC, r), which can be calculated using:

$$r=\frac{\sum_{i=1}^{n}\left(x_i-\overline{x}\right)\left(y_i-\overline{y}\right)}{\sqrt{\sum_{i=1}^{n}\left(x_i-\overline{x}\right)^2\sum_{i=1}^{n}\left(y_i-\overline{y}\right)^2}}; \tag{14}$$

(4) Scatter index (SI, $s_{\rm i}$), which can be calculated using:

$$s_{\rm i}=\frac{1}{\overline{x}}\sqrt{\frac{1}{n}\sum_{i=1}^{n}\left[\left(y_i-\overline{y}\right)-\left(x_i-\overline{x}\right)\right]^2}. \tag{15}$$

In Eqs (12)–(15) x_i denotes the zero-crossing mean period ($T_{\rm z}$) from the ERA-Interim; y_i denotes $T_{\rm z}$ from the inversion models; $\overline{x}$ and $\overline{y}$ denote the zero-crossing mean wave period from the ERA-Interim and the inversion models respectively; and n is number of samples. These indexes are mainly used to express degree of deviation and correlation between inversion results and true values and can express an inversion accuracy well. In Fig. 2, the different colors represent the sample density. The samples in Fig. 2b are the closest to the central line and the densest around the central line. This result indicates that these samples are the best inversion results. Thus, the inversion of zero-crossing mean wave period using the PQP-AVISO-model has the highest precision of the six models. Several accuracy indicators for the PQP-AVISO-model are the best, i.e., the bias is –0.27 s, the RMSE is 0.86 s and the scatter index SI is 0.15. Moreover, the inversion accuracies of the PQ-AVISO-model and the MWP-NN-model are also higher than the Miao-QP-model, the Miao-PQP-model and the H98-model. Therefore, the PQP-AVISO-model is the most suitable for zero-crossing mean wave period inversions in the China's seas. The values of zero-crossing mean wave period for each grid point were calculated using the PQP-AVISO-model from September 2009 to August 2013.

4 Wave energy actual application value

The actual application value of a wave power project is important to consider before constructing a wave power farm. The annual effective energies $E_{\rm e}$ ($E_{\rm e}$=$P_{\rm w}$×365×24×$U_{H_{\rm s}}$, $U_{H_{\rm s}}$ is the frequency of the significant wave height being greater or equal to 0.5 m, which is the effective wave power per unit wave front; Zheng and Lin et al., 2013) at Stas kzscd, 010 and kzszs were used to analyze the value of the wave power farms constructed in these locations. Satisfying the power demands of island residents was considered the goal of the wave power farms in nearshore waters. According to the Shandong Statistical Information Net and the Zhejiang Provincial Bureau of Statistics Net, the annual per capital power consumptions in the areas adjacent to these three buoy stations are 487, 676 and 716 kW·h, respectively. The average power consumption is 626 kW·h, which can be used as an index of per capital power consumption. Power supply ability for a residential electricity consumption in adjacent islands from the wave energy per 1 km wave front a at three buoy stations are illustrated in Table 3. At Sta. kzscd, the wave energy can provide an annual power consumption of 16 800 people (39% of the total population) in Changdao County. The available energy at Sta. 010 is equivalent to an annual power consumption of 24 000 people. Station 010 is adjacent to Lingshan Island, which has a population of approximately 2 700. Thus, the available energy in this area can provide approximately 9 years of power for residents, which is valuable on Lingshan Island where energy resources are scarce. At Sta. kzszs, the available energy is equivalent to an annual power consumption of 95 700 people in the Zhoushan Islands. Therefore, the wave energy resources should be efficient supplemental source of energy for these areas, and the utilization of the wave energy should reduce the consumption of the conventional energy.

Table 3. Wave energy actual application value statistics at three buoy stations

Buoy station ID	Adjacent island	Available energy/ GW·h·a^{-1}·km^{-1}	Power supply ability/10^4·a^{-1}
kzscd	Changdao Island	10.548	1.68
010	Lingshan Island	15.003	2.40
kzszs	Zhoushan Islands	59.912	9.57

5 Wave energy assessments in offshore areas of China

The significant wave height and wind speed data for four recent years in the China's seas were from the AVISO multi-satellite merged altimeter data; zero-crossing mean wave period values were subsequently calculated using the PQP-AVISO-model and converted to determine energy period. On the basis of the acquired wave data and the WD-model, we calculated $P_{\rm w}$ and several evaluation indexes and assessed the wave energy resources in offshore areas of China.

5.1 *Characteristics of wave energy resources*

The annual average and seasonal average $P_{\rm w}$ distributions that were calculated from the altimeter data are shown in Fig. 3. Pronounced regional and seasonal variations in the wave power density are present in the China's seas. The areas with large $P_{\rm w}$ values (approximately 14.0–18.5 kW/m) are primarily located in the north-central part of the South China Sea, the Luzon Strait,

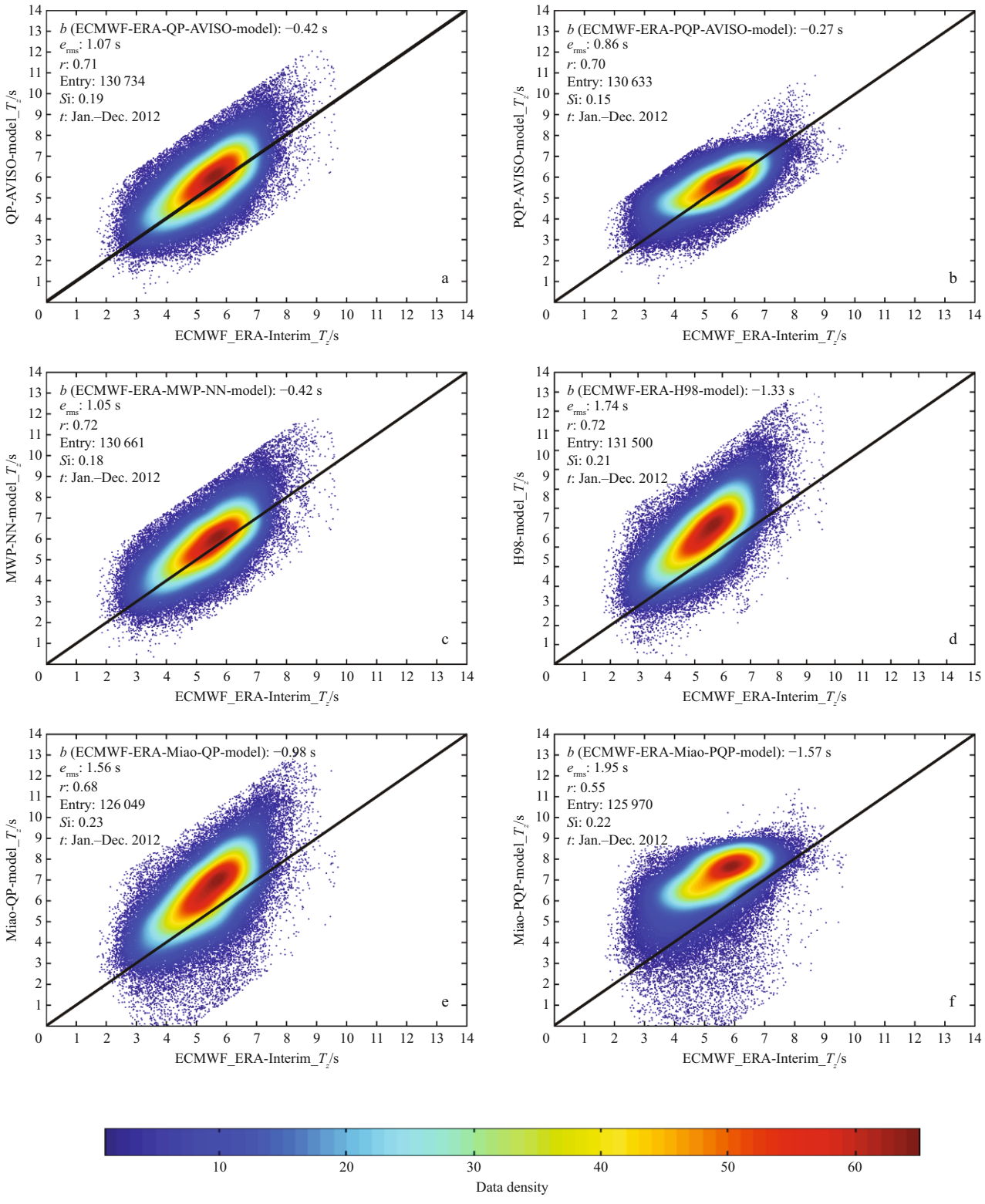

Fig. 2. Scatter plots of zero-crossing mean wave period calculated using the QP-AVISO-model (a), the PQP-AVISO-model (b), the MWP-NN-model (c), the H98-model (d), the Miao-QP-model (e) and the Miao-PQP-model (f) versus zero-crossing mean wave period from the ECMWF ERA-Interim dataset

east of Taiwan, China and the Philippines. Because the wave energy resources are affected by the East Asia monsoon, these resources exhibit pronounced differences in their seasonal distributions. The P_w values are the largest in all areas of the China's seas in winter because of cold waves and gales that are caused by the northeast monsoon. Specifically, the P_w values are 1–9 kW/m in the Bohai Sea and the Yellow Sea and 9–16 kW/m in the East China Sea. Large P_w values (approximately 22–27 kW/m)

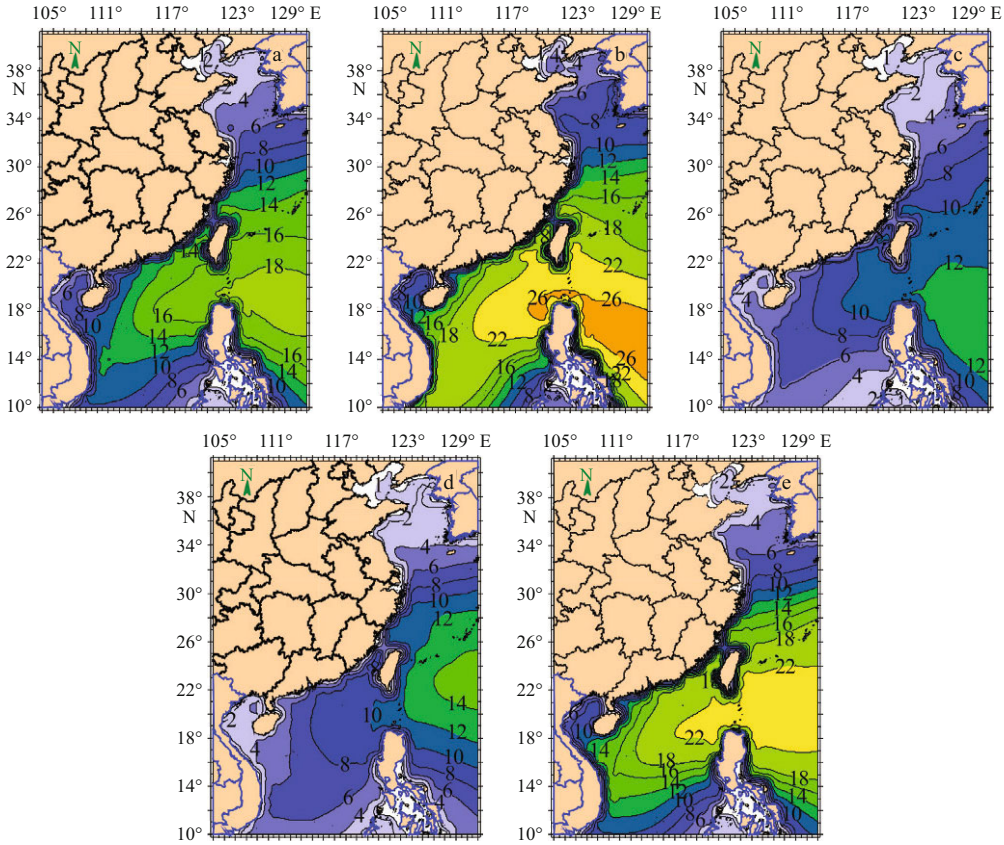

Fig. 3. Multiyear mean wave power density (kW/m) distributions: annual (a), winter (b), spring (c), summer (d) and autumn (e).

are located in the central part of the South China Sea, the Luzon Strait and east of the Philippines. Because of the effects of the ocean weather, the P_w values are the smallest (1–9 kW/m) in the Bohai Sea, the Yellow Sea and the East China Sea in spring. The P_w values near Taiwan decrease to 10 kW/m; the areas of large P_w values are located in northeast of the Philippines. The P_w distributions in most areas of the China's seas in summer are similar to those in spring because the monsoon is relatively weak. In summer, the areas of large P_w values (12–15 kW/m) move from northeast of the Philippines to near the Ryukyu Islands because of tropical storms. In autumn, a Mongolian high pressure is regenerated. The P_w values in most areas of the China's seas are slightly lower (approximately 2–4 kW/m) less than those in winter, and the P_w values in the East China Sea and the Beibu Gulf remain the same. These results are consistent with those of Zheng and Pan et al. (2013) and Zheng and Li (2011).

5.2 *Richness of wave energy resources*

The richness of wave energy resources is an important factor in identifying ideal locations for wave power plants. Ren et al. (2008), Ren et al. (2009) and Zheng and Pan et al. (2013) indicated that wave energy is available when $P_w \geqslant 2$ kW/m and is rich when $P_w \geqslant 20$ kW/m. In this paper, the frequencies of $P_w \geqslant 2$ kW/m and $P_w \geqslant 20$ kW/m, which are called the usable level frequency (ULF) and the rich level frequency (RLF), respectively, were calculated using the altimeter data (Fig. 4). The Bohai Sea has the smallest ULF (less than 40%). Moreover, the Yellow Sea has ULF values of 40%–80%, and more than 70% of the East China Sea and the South China Sea contains areas of $P_w \geqslant 2$ kw/m throughout the year. Large ULF areas are primarily located in the southern part of the East China Sea, the northeastern part of the South China Sea, the Luzon Strait and east and southeast of Taiwan. The RLFs in the Bohai Sea and the Yellow Sea are small (less than 6%), and the RLFs in the East China Sea are between 10% and 15%. Large areas of RLF are primarily located in the central part of the South China Sea, the Luzon Strait and east and southeast of Taiwan; however, the frequencies are less than 33%. In general, most areas of the China's seas do not contain rich wave energy resources; however, the wave energy is available. These results are similar to the findings of Zheng and Pan et al. (2013), while the values presented in this study are higher, which is most likely due to the differences in significant wave

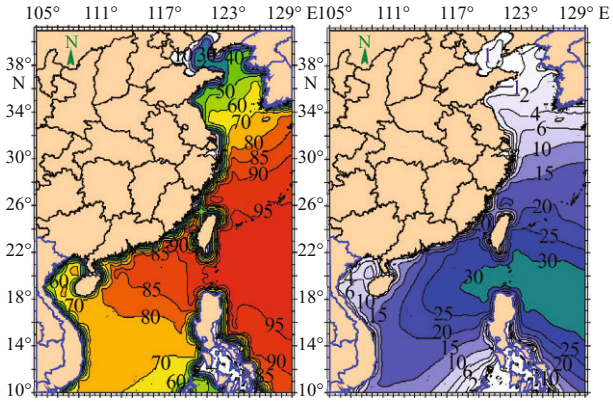

Fig. 4. Distributions of energy level frequency (%). a. ULF and b. RLF.

height.

5.3 *Stability of wave energy resources*

Cornett (2008) found that the wave energy variation (stability) is an important factor that affects the feasibility of wave energy resource exploitation projects. The wave energy stability is more important than the wave energy reserves, and a stable energy is advantageous for exploitation and utilization. The wave energy stability is quantified via several indexes, such as the coefficient of variation (COV), i.e., $\mathrm{COV}=\sqrt{(1/N)\cdot\sum_{i=1}^{N}(P_w-\overline{P_w})^2}/\overline{P_w}$, the seasonal variability index (SV), i.e., $\mathrm{SV}=(P_{s1}-P_{s4})/P_{year}$, and the monthly variability index (MV), i.e., $\mathrm{MV}=(P_{M1}-P_{M12})/P_{year}$, where $\overline{P_w}$ is the mean wave power density, P_{s1} and P_{s4} are the maximum and minimum seasonal mean wave power densities, respectively, P_{M1} and P_{M12} are the maximum and minimum monthly mean wave power densities, respectively, and P_{year} is the annual mean wave power density. Higher index values indicate larger wave energy variations and decreased stability compared with lower index values.

The COV, SV and MV of P_w were calculated from four years of AVISO altimeter data. The COV, SV and MV distributions are shown in Fig. 5 and indicate that the wave energy stability is relatively poor in the Bohai Sea, the Yellow Sea, the southwest part of the South China Sea and east and south of the Philippines. The COV, SV and MV values in most areas of the Bohai Sea are greater than 1.4, 1.0 and 1.6, respectively. In most areas of the Yellow Sea, the COV values are 1.2–1.6, the SV values are 0.6–1.0 and the MV values are 1.0–1.6; the monthly variation is significant. In the southwest part of the South China Sea, the COV values are generally greater than 1.2, the SV values are greater than 1.0 and the MV values are greater than 1.6, which is similar to the oceanic region that is located east and south of the Philippines. The East China Sea and the waters northeast of Taiwan are areas of relatively stable wave energy, which is especially reflected in the seasonal and monthly variations, where the SV and MV values are less than 0.6 and 1.2, respectively. The wave energy is relatively stable in the north-central part of the South China Sea, the Luzon Strait and the waters east and south of Taiwan. These results are consistent with those of Cornett (2008); however, the values presented herein are slightly smaller.

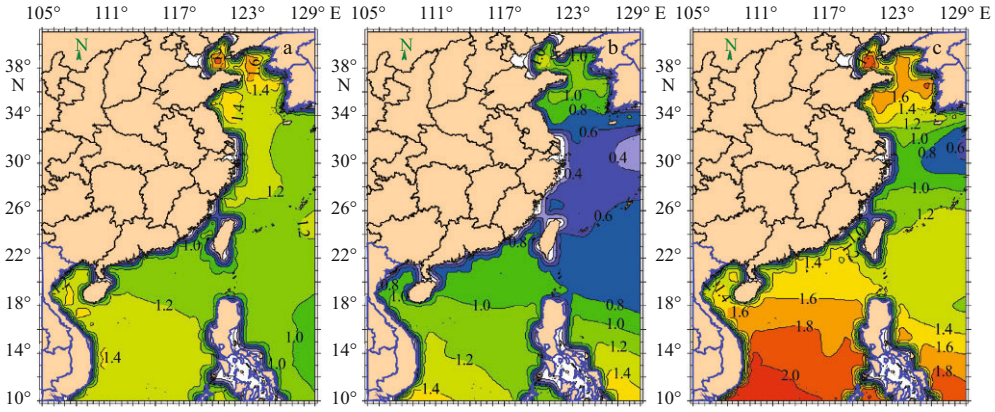

Fig. 5. Stability index distributions. a. COV, b. SV and c. MV.

5.4 *Total wave energy and its seasonal variation*

The wave energy reserve is also one of important factors for wave energy assessment in typical areas. In this study, the total wave energy is defined to denote reserve. A synoptics method and a climatology method are two main methods for the total wave energy calculation in recent years (Li et al., 1984; Ma and Yu, 1983) in which the climatology method is a better choice because a long-term average is used in this method which can present a long-term trend. The process of the climatology method is as follows: first, the wave energy density ($\overline{E}$) which can be calculated using Eq. (4) is calculated for each grid; then wave energy is equal to wave energy density multiplying area for each grid. The total wave energy is the sum of the wave energy for each grid. In this paper, using the climatology method and the AVISO data, four seasonal total wave energy are calculated for the China's seas and shown in Fig. 6. The total wave energy in winter, spring, summer and autumn are 9.2166, 3.9819, 3.6547, 7.2839 PJ respectively. Pronounced seasonal variations in the total wave energy are also present in the China's seas. The total wave energy is larger in winter and autumn than at in spring and summer; so the wave energy exploitation is mainly in winter and autumn.

5.5 *Distribution of total wave energy density according to wave state*

When assessing the wave energy, we also need consider the actual demand for the WECs. The evaluating indexes must combine with the WECs. So several factors that affect the design of WECs must be further examined. Several studies have shown that the wave height and the wave period are two important parameters for determining the component dimensions in pneumatic WECs, Isaacs wave energy pumps and Kayser wave ener-

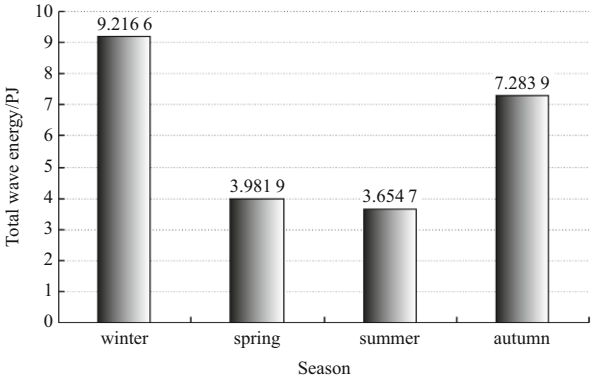

Fig. 6. Total wave energy in four season.

gy generators (Li et al., 1984).

In this study, we focus on the distribution of the total wave energy density (the mean of the sum of P_w multiplied by the number of hours in a year (MW·h/(m·a)) according to the wave state which can be used to design the WECs to improve the utilization ratio of wave energy resources. From 4 years of the AVISO altimeter data, the ratio of the total wave energy density with 0.5 m≤significant wave height≤4 m, 4 s≤energy period≤10 s to total wave energy density with all wave state were calculated to determine the distribution of total wave energy density according to the wave state in the China's seas which is shown in Fig. 7. As shown in Fig. 7, except for very coastal waters, in other sea areas in the China's seas, the energy are primarily from wave state with 0.5 m≤significant wave height≤4 m, 4 s≤energy period≤10 s; within this wave state, the wave energy accounts for 80% above of total wave energy. This characteristic is advantageous to designing the WECs. The WECs can be commonly used in all areas, have higher wave energy availability and reduce effectively the cost of design and construction for the WECs if they are designed to accommodate the range of dominant wave states identified by the above described criteria.

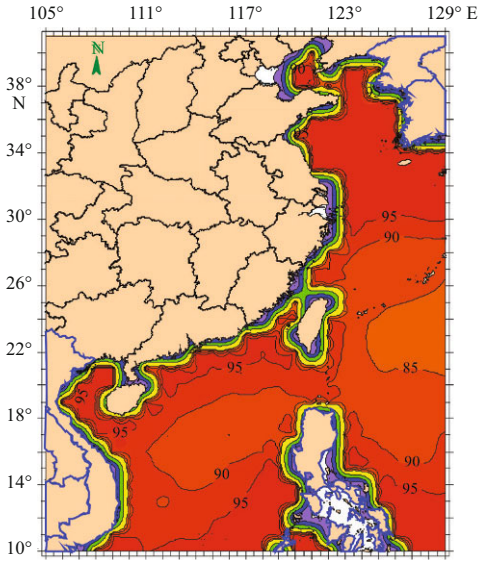

Fig. 7. Distribution of total wave energy (%) according to wave state.

6 Conclusions

Wave energy resources were assessed for the China's seas based on an AVISO altimeter wave data set. The conclusions of this study are as follows.

(1) A parameterized model of the wave power density that considers the effects of the water depth was introduced (the WD-model). Several comparisons between the WD-model and the EM-model were performed based on buoy data. The results show that the EM-model underestimates the wave power density and that the underestimation increases with increasing wave conditions, which has a large effect on the total wave energy reserves.

(2) On the basis of the relationship between the nondimensional wave height and the wave age, three novel mean wave period inversion models were established using the AVISO data and the ERA-Interim data, including the QP-AVISO-model, the PQP-AVISO-model and the MWP-NN-model. The PQP-AVISO-model is the best model and is suitable for mean wave period inversions in the China's seas.

(3) The wave energy resources were assessed in the China's seas for the first time using the altimeter wave observation data set. The results indicate that pronounced regional and seasonal variations in the wave power density are present in the China's seas. Areas of large P_w values (approximately 14.0–18.5 kW/m) are located in the north-central part of the South China Sea, the Luzon Strait and east of Taiwan and the Philippines. The distribution of the wave energy resources also has seasonal differences due to the East Asia monsoon. The wave energy is abundant in autumn and winter and poor in spring and summer. The Bohai Sea has the smallest ULF area. However, the Yellow Sea has the ULFs that are also small. The East China Sea and the South China Sea have higher ULFs, i.e., greater than 70% throughout the year. Areas of high ULFs are located in the south part of the East China Sea, the northeast part of the South China Sea, the Luzon Strait and east and southeast of Taiwan. The East China Sea and the waters northeast of Taiwan are relatively stable areas of the wave energy with SV values less than 0.6 and MV values less than 1.2. Pronounced seasonal variations in the total wave energy are also present in the China's seas. The wave energy exploitation is mainly in winter and autumn. In addition, except for very coastal waters, in other sea areas in the China's seas, the energy is primarily from wave state with 0.5 m≤significant wave height≤4 m, 4 s≤energy period≤10 s; within this wave state, the wave energy accounts for 80% above of the total wave energy. This characteristic is advantageous to designing the WECs. The results are consistent with other studies, indicating that this novel observation method using altimeters is valid for assessing the wave energy in the China's seas.

(4) The wave energy resource should be an efficient supplemental source of energy for some areas, and the utilization of the wave energy should reduce the consumption of the conventional energy.

Acknowledgement

The authors would like to thank the CNES and the CLS for providing the AVISO multi-satellite merged altimeter data sets, the ECMWF for providing the ERA-Interim data sets and the Ocean Renewable Energy Special Fund Project of the State Oceanic Administration, China (GHME) for providing the buoy data.

References

Abdalla S, Janssen P, Bidlot J. 2008. OSTST 2008 Meeting: Jason-2 Wind and Wave Products: Monitoring, Validation and Assimilation AVISO and PODAAC User Handbook. 2008. IGDR and GDR Jason Products, SMM-MU-M5-OP-13184-CN (AVISO), 4.1ed. France: CNES and CLS

Arinaga R A, Cheung K F. 2012. Atlas of global wave energy from 10 years of reanalysis and hindcast data. Renewable Energy, 39(1): 49–64

Bai Shaocheng. 2006. A brief analysis of the world energy crisis and China's strategic solution. Experiment Science & Technology (in Chinese), (Z1): 168–170

Barstow S, Haug O, Krogstad H. 1998. Satellite altimeter data in wave energy studies. In: Proceedings of Waves'97. Skudai: Universiti Teknologi Malaysia, 339–354

Challenor P G, Srokosz M A. 1991. Wave studies with the radar altimeter. Int J Remote Sens, 12(8): 1671–1686

CNES, CLS. 2010. High-precision altimetry with satellites working together. http://www.aviso.altimetry.fr/en/techniques/altimetry/multi-satellites.html

Cornett A M. 2008. A global wave energy resource assessment. In: Pro-

ceedings of 18th International Conference on Offshore and Polar Engineering. BC, Canada, Vancouver: The International Society of Offshore and Polar Engineers
ECMWF. 2013. User Guide to ECMWF Forecast Products. UK, Reading: ECMWF
Folley M, Whittaker T J T. 2009. Analysis of the nearshore wave energy resource. Renewable Energy, 34(7): 1709–1715
Gommenginger C P, Srokosz M A, Challenor P G, et al. 2003. Measuring ocean wave period with satellite altimeters: a simple empirical model. Geophysical Research Letters, 30(22): 2150
Guan Yi. 2011. Study on feasibility evaluation of wave energy in China (in Chinese)[dissertation]. Qingdao: Ocean University of China
Hsu T W, Liau J M, Lin J G, et al. 2012. Sequential assimilation in the wind wave model for simulations of typhoon events around Taiwan Island. Ocean Engineering, 38(2–3): 456–467
Hwang P A, Teague W J, Jacobs G A, et al. 1998. A statistical comparison of wind speed, wave height, and wave period derived from satellite altimeters and ocean buoys in the Gulf of Mexico region. J Geophys Res, 103(C5): 10451–10468
Iglesias G, López M, Carballo R, et al. 2009. Wave energy potential in Galicia (NW Spain). Renewable Energy, 34(11): 2323–2333
Li Luping, Tian Suzhen, Xu Shenglai, et al. 1984. Power resource estimation of ocean surface waves in the Bohai Sea and Huanghai Sea and an evalution of prospects for converting wave power. Journal of Oceanography of Huanghai & Bohai Seas (in Chinese), 2(2): 14–23
Li Chengkui, Liao Wenjun, Wang Yuxin. 2010. Research progress of ocean wave energy power technology in the world. The Magazine on Equipment Machine (in Chinese), (2): 68–73
Li Ruili. 2007. Research on various periods of sea waves (in Chinese) [dissertation]. Qingdao: Ocean University of China
Ma Huaishu, Yu Qingwu. 1983. The preliminary estimate for the potential surface wave surface wave energy resources in the adjacent sea areas of China. Marine Science Bulletin (in Chinese), 2(3): 73–82
Mackay E B L, Retzler C H, Challenor P G, et al. 2008. A parametric model for ocean wave period from Ku band altimeter data. J Geophys Res, 113(C3): C03029
Miao Hongli, Ren Haoran, Zhou Xiaoguang, et al. 2012. Study on altimeter-based inversion model of mean wave period. Journal of Applied Remote Sensing, 6(1): 063591
Pontes M T. 1998. Assessing the European wave energy resource. Journal of Offshore Mechanics and Arctic Engineering, 120(4): 226–231
Pontes M T, Aguiar R, Oliveira Pires H. 2005. A nearshore wave energy atlas for Portugal. Journal of Offshore Mechanics and Arctic Engineering, 127(3): 249–255
Pontes M T, Bruck M. 2008. Using remote sensed data for wave energy resource assessment. In: Proceedings of the ASME 27th International Conference on Offshore Mechanics and Arctic Engineering. ASME, Portugal, Estoril, 1–9
Queffeulou P, Bentamy A, Croizé-Fillon D. 2010. OSTST 2010 Meeting: Validation Status of a Global Altimeter Wind & Wave Data Base. Portugal, Lisbon: CNES
Quayle R G, Changery M J. 1981. Estimates of coastal deepwater wave energy potential for the world. In: Proceedings of Conference of Oceans 1981. Boston, MA: IEEE, 903–907
Quilfen Y, Chapron B, Collard F, et al. 2004. Calibration/validation of an altimeter wave period model and application to TOPEX/Poseidon and Jason-1 altimeters. Mar Geodesy, 27(3–4): 535–549
Ren Jianli, Luo Yuya, Chen Junjie, et al. 2009. Research on wave power application by the information system for ocean wave resources evaluation. Renewable Energy (in Chinese), 27(3): 93–97
Ren Jianli, Luo Yuya, Zhong Yingjie, et al. 2008. The implementation for the analysis system of ocean wave resources and the application of wave energy power generation. Journal of Zhejiang University of Technology (in Chinese), 36(2): 186–191
Smith W H F, Sandwell D T. 1997. Global sea floor topography from satellite altimetry and ship depth soundings. Science, 277(5334): 1956–1962
Stopa J E, Cheung K F, Chen Yileng. 2011. Assessment of wave energy resources in Hawaii. Renewable Energy, 36(2): 554–567
Wang Chuankun. 1984. Wave energy preliminary analysis for the Chinese coastal waters. Donghai Marine Science (in Chinese), 2(2): 32–38
Wang Chuankun, Lu Dechao. 1989. Ocean Energy Resources Zoning for Chinese Coastal Countryside (in Chinese). China: Science and Technology Division of State Oceanic Administration, Science and Technology Division of Hydroelectric Department
Wang Chuankun, Lu Wei. 2009. Analysis Methods and Reserves Evaluation of Ocean Energy Resources (in Chinese). Beijing: China Ocean Press, 61–62
Wen Shengchang, Yu Zhouwen. 1985. Ocean Wave Theory and Calculation Principle (in Chinese). Beijing: China Science Press, 203–204
Wang Xifeng. 2006. Research on Retrieving Wave Period from Satellite Altimeters (in Chinese) [dissertation]. Qingdao: Ocean University of China
Yang Le. 2009. Satellite radar altimeter remote sensing inversion algorithm research in the coastal water of China and high sea state (in Chinese) [dissertation]. Nanjing: Nanjing University of Science and Technology
Zheng Chongwei, Li Xunqiang. 2011. Wave energy resources assessment in the China Sea during the last 22 years by using WAVEWATCH-III wave model. Periodical of Ocean University of China (in Chinese), 41(11): 5–12
Zheng Chongwei, Lin Gang, Shao Longtan. 2013. Wave energy resources analysis around Taiwan waters. Journal of Natural Resources (in Chinese), 28(7):1179–1186
Zheng Chongwei, Pan Jing. 2014. Assessment of the global ocean wind energy resource. Renewable and Sustainable Energy Reviews, 33: 382–391
Zheng Chongwei, Pan Jing, Li Jiaxun. 2013. Assessing the China Sea wind energy and wave energy resources from 1988 to 2009. Ocean Engineering, 65: 39–48
Zheng Chongwei, Shao Longtan, Shi Wenli, et al. 2014. An assessment of global ocean wave energy resources over the last 45 a. Acta Oceanologica Sinica, 33(1): 92–101
Zheng Chongwei, Su Qin, Liu Tiejun. 2013. Wave energy resources assessment and dominant area evaluation in the China Sea from 1988 to 2010. Haiyang Xuebao (in Chinese), 35(3): 104–111
Zheng Chongwei, Zheng Yuyan, Chen Hongchun. 2011. Research on wave energy resources in the northern South China Sea during recent 10 years using SWAN wave model. Journal of Subtropical Resources and Environment (in Chinese), 6(2): 54–59
Zheng Chongwei, Zhuang Hui, Li Xin, et al. 2012. Wind energy and wave energy resources assessment in the East China Sea and South China Sea. Science China: Technological Sciences, 55(1): 163–173